Journal of Harbin Engineering University
ISSN: 1006-7043

Vol 47 No. 03
March 2026

Deep Embedded Clustering-Based Bounding Box Detection for Enhanced Object Recognition in Remote Sensing Aerial Images

Shalini L[1], Dr. Thirupurasundari D R[2]

[1, 2] Department of Computer Science and Engineering, Bharath Institute of Higher Education and Research, Chennai, Tamil Nadu

Email Id: [1] shalini.cse@bharathuniv.ac.in, [2] thirupurasundari.cse@bharathuniv.ac.in

Abstract

Aerial image analysis through remote sensing is an important tool in urban planning as well as environmental surveillance, but the correct identification of objects is challenging because of different scales, occlusions, and background clutters. Old object detectors have the problem of low detection and high rates of false detection. In order to eliminate these restrictions, this paper presents a Deep Embedded Clustering (DEC)-based bounding box detection algorithm. The system combines hybrid clustering and multi-scale feature representation to enhance the detection of objects of different sizes in complicated aerial scenes. A pre-trained CNN is then used to extract high-dimensional features and they are then clustered based on a KL divergence loss. In the clustering module, the positions of bounding boxes are refined at any dynamic time by weighted adjustment of centroid positions, which enhances the accuracy of localization. The framework greatly improves accuracy and recalls by lowering the false detections and improving feature separability. The experimental assessment shows that its accuracy is 94.7% with a 15% false-positives decrease, which is better than existing detectors, including YOLOv5, Faster R-CNN and SSD.

Keywords: Deep Embedded Clustering, Bounding Box Detection, Remote Sensing, Object Recognition, Aerial Images.

1. Introduction

Aerial remote sensing images are becoming a critical element in environmental surveillance, city planning, management of disasters and military surveillance. Determining the roads, buildings, and cars is possible with the help of high-resolution images that allow protecting a wide geographic region (Gui et al., 2024; Antonakakis et al., 2023). As the drone and satellite imagery has been made more open, machine learning has become fundamental in automation of object detection. Nonetheless, the limitation of the detection is due to factors like differing scales, occlusions, and cluttered backgrounds. Traditional sliding-window methods and feature-based model (Anuar et al., 2022) are prone to failure in low-contrast or noisy conditions, which encouraged deep learning-based studies to achieve robust object localization and classification.

A. Challenges

The challenges of CNN-based localization include aerial images that are characterized by scale and rotation, leading to impediments (Gui et al., 2024). False positives occur when there is complex backgrounds vegetation, shadows, or water bodies whereas false negatives occur when occlusions occur due to natural and man-made structures. Besides, the mass surveillance needs lightweight but precise models that can operate with significant volumes of data with a minimal amount of resources (Rajput et al., 2024; Praghas et al., 2022; Kalinicheva et al., 2020).

B. Problem Definition

The traditional models (Faster R-CNN, SSD, YOLOv5) are effective on natural images but fail in aerial conditions because of the complexity of the background and the changes in scale (Sharma et al., 2024; Lin et al., 2021). Also, the clustering-based methods that use unsupervised learning tend to misalign bounding boxes. Hybrid-type deep clustering CNN can enhance the localization as well as classification accuracy.

C. Objectives

The Main Contributions are:

1. To establish a strong bounding box detecting algorithm using DEC to detect objects accurately in a remote sensing aerial image.

2. To enhance object localization and classification through the hybridization of clustering and multi-scale feature extraction; therefore, it will enhance the robustness of the framework to real-world remote sensing.
3. To enhance performance of object detection and object recall with a reduction in false positives and an increase in the correspondence between the predicted and real object boundaries on the predicted bounding box.

The suggested DEC based framework combines soft clustering, CNN features and uses KL divergence and IoU-driven refinement to refine the bounding boxes to have more precise and reduce overlaps and improve the accuracy of detection in complicated aerial images.

2. Literature Survey

Object detection using histogram of oriented gradients (HOG) and scale-invariant feature transform (SIFT) has been used but is reported to be limited by clouding and lighting (Zheng et al., 2023). Though it is accurate, Faster R-CNN can not detect objects with high-resolution aerial because of the computational complexity, particularly in real-time. SSD is efficient but not effective in identifying small objects due to fixed grid sizes (Alhawsawi et al., 2024). YOLOv5 is faster with one pass network, but with poor performance on complex backgrounds and small object detection. DEC has shown itself to be effective in high-dimensional clustering, but has not been directly useful in detection (Lago et al., 2024). The combination of DEC and CNN-based feature extractors can be used to improve detection quality and bounding box optimization in aerial scenes.

Current advances in deep learning have greatly enhanced the aerial object detection but problems such as dense backgrounds and small objects remain (Wang et al., 2023). YOLOv7 and the wider YOLO family proposed trainable bag-of-freebies and re-parameterization strategies and struck a new tradeoff between speed and accuracy. This is extended to the UAV-based tasks by lightweight successors like YOLOv8n, which can still perform under limited resources (Yue et al., 2024).

Models based on transformers have also contributed to detection by localizing global dependencies. DETR model had initial convergence and tiny object problems (Carion et al.). Multi-scale deformable attention was used by deformable DETR to solve this issue, and enhance performance on dense aerial scenes (Zhang et al., 2022). DINO was later improved with denoising anchor boxes and mixed query selection, and instability problems were solved (Zhu et al., 2020). Also, the hierarchical feature representation has been offered by Swin Transformer with shifted window partitioning, which has been shown to be efficient in dense prediction and aerial tasks (Liu et al., 2021).

A gap exists on cohesive detection-to-decision systems that integrate real-time aerial sensing, secure data provenance, and smart analytics of transparent and safe agri-food supply chain monitoring. In spite of these advancements, such problems as false positives and precision of the bounding box persist. DEC-enhanced detection offers a trade-off between lightweight CNN performance and transformer accuracy by use of clustering in feature space to give refinement to localization, reduce false positives, and detect small objects

3. Methodology

To enhance object localization and classification in remote sensing aerial images, the proposed bounding box detection method based on DEC integrates feature extraction and clustering. Fig. 1 shows the system flow of proposed work.

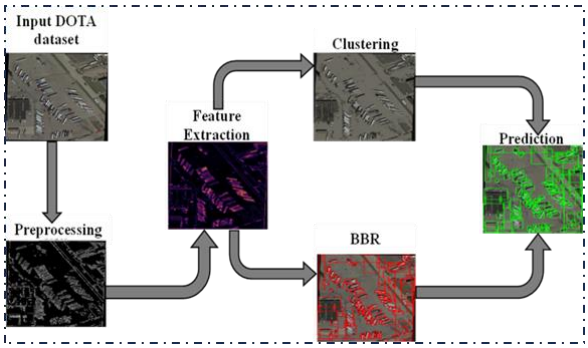

Fig. 1. System Model

The pipeline involves preprocessing images using noise reduction filters, edge detection and Sobel gradients, and KMeans clustering to separate vehicles and background, and refined bounding boxes to create optimized and specific classifications.

A. Data Preprocessing

Preprocessing stage guarantees that of aerial images being clean and standardized. Gaussian filtering is used to minimize noise, histogram equalization is used to increase contrast, and the intensities of pixels are normalized. Photos are resized to standard size, and Canny edges are detected to highlight the contours,

enhancing the feature identification and proper object localization as CNN input

B. Feature Extraction

Convolutional Neural Networks (CNN's) serves in target Feature extraction is performed using a CNN to identify patterns and object characteristics from aerial images. It has convolutional layers of 3-by-3 kernel Parameters and ReLU activation to seek features, and the layer of max pooling to decrease the density dimensions. The final layer of the network has 256 fully connected neurons with ReLU as the high-level feature representation layer.

C. Clustering-Enhanced Feature Selection and Bounding Box Refinement

The suggested solution improves object detection in aerial images as it includes DEC and bounding box regression. The CNN extracted feature vectors go through a DEC module which calculates soft cluster assignments with a student's t-distribution to determine similarity between data points and centers. The clustering loss is computed as the KL divergence between the predicted cluster distribution qi and the target distribution p_i:

$$L_c = \sum_i KL(p_i||q_i) = \sum_i p_i \, log\frac{p_i}{q_i} \quad (1)$$

The cluster assignments are dynamically updated using centroid re-weighting, improving object localization and reducing false positives.

a. Clustering Assignment

The code vectors that capture texture, shape and edge information are projected into a latent space with a fully connected layer. The similarity score between a sample z_i and a centroid μ_j is computed as:

$$q_{i,j} = \frac{(1+||z_i-\mu_j||^2/\alpha)^{-\frac{\alpha+1}{2}}}{\sum_k(1+||z_i-\mu_k||^2/\alpha)^{-\frac{\alpha+1}{2}}} \quad (2)$$

where:

$q_{i,j}$ = probability of sample i belonging to cluster j; z_i = latent space representation of the feature vector; μ_j = centroid of cluster j; α = degrees of freedom (set to 1 for t-distribution)

b. Clustering Loss Calculation

The clustering loss is computed using the KL divergence between the predicted cluster distribution q_i and the target distribution p_i. The target distribution is computed based on the high-confidence samples using the following equation:

$$p_{i,j} = \frac{q_{i,j}^2/\sum_i q_{i,j}}{\sum_k(q_{i,k}^2/\sum_i q_{i,k})} \quad (3)$$

where:

$p_{i,j}$ = target distribution for sample i and cluster j; $q_{i,j}$ = predicted cluster assignment

The target distribution increases the contribution of high-confidence samples while suppressing noisy predictions.

c. DEC Loss with Bounding Box Refinement

To strengthen spatial alignment, clustering loss is combined with IoU-based bounding box regression The objective function may be formulated as:

$$\mathcal{L}_{DEC} = KL(P||Q) + \lambda \cdot \mathcal{L}_{IoU} \quad (4)$$

where:

P represents the target distribution derived from soft cluster assignments; Q is the predicted probability distribution over clusters; $\mathcal{L}_{IoU}$ is the generalized IoU loss. The balancing term λ ensures that feature space clustering and geometric alignment contribute jointly.

d. Bounding Box Refinement

Bounding box regression modifies CNN-predicted coordination. Refinement also has centroid adjustment. The bounding box is adjusted using the weighted centroid information from the clustering assignment:

$$B_r = B_{\text{init}} + \beta \cdot (\mu_c - z_i) \quad (5)$$

where:

B_r = refined bounding box coordinates; β = adjustment coefficient (set to 0.1); μ_c = cluster centroid; z_i = feature vector

Non-Maximum Suppression (NMS): Overlapping bounding boxes are resolved using NMS, which retains the box with the highest confidence score and discards others with an IoU higher than 0.5.

i. Training Strategy

The training loss combines clustering and bounding box components. The total loss for training is computed as:

$$L_t = \lambda_1 L_c + \lambda_2 L_{\text{bbox}} \quad (6)$$

where:

λ_1 and λ_2 = weight coefficients for clustering and bounding box loss (set to 0.5 and 1.0 respectively). This ensures joint optimization of cluster assignments and bounding box accuracy.

ii. Prediction Phase

The test images undergo CNN layers (3 X 3 convolutions, ReLU activations, max pooling). The feature vectors are projected into latent space, clustered, and bounding boxes predicted. Refinement modulates coordinates based on centroid similarity, whereas confidence scores provide robust detection. The end results are refined using NMS, which results in sound localization of objects.

4. Results and Discussion

The model is implemented using Python with TensorFlow and Keras libraries. It uses the acceleration of GPUs to access the large-scale aerial images data sets. Data augmentation is implemented to improve the model strength against scale, orientation, and light variations. Table 1 represents the experimental setup includes parameters and values.

Table 1: Experimental Setup

Parameter	**Value**
Image Size	512 × 512 pixels
Batch Size	32
Learning Rate	0.0001
Epochs	100
Optimizer	Adam
Loss Function	Cross-Entropy + KL Divergence
GPU Used	NVIDIA RTX 3090 (24 GB VRAM)

The DOTA dataset is a massive reference on object detection in the aerial image. It has more than 190,000 annotated objects of more than 2,800 images (15 categories, including vehicles, buildings and ships). The data set has varying resolutions, orientations and complicated backgrounds as is the case in real world situation.

A. Implementation Outcomes

This section discusses the results of the implementation. The performance metrics with which the proposed model is analyzed to determine its effectiveness are different.

Fig. 2 depicts grouping of features by the proposed DEC framework. In the two-dimensional feature space, which has been simplified for visualization, the various classes of objects cars (red), buildings (blue), and ships (green) are clustered into compact and highly separated groups. DEC makes sure to pull features of the same category closer together and maximize the inter-class separability.

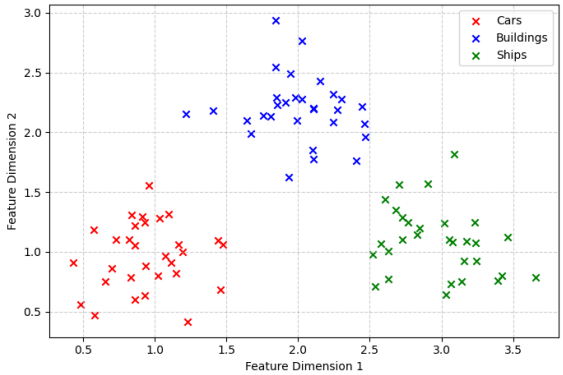

Fig. 2. Feature clustering using DEC

Fig. 3 demonstrate the bounding box refinement by comparing predicted boxes with ground truth boxes. The x and y-axis indicate the pixel location in the image where x is horizontal and y is vertical. In this only uses two objects, but the refinement procedure can be run over the entire data set, fitted increasingly accurate predicted boxes to ground truth using cluster centroid and optimization of IoU. This refinement eliminates localization errors, minimizes redundancies, and increases the reliability of detections, especially in dense aerial scenes, where small localization errors can lead to either false positives or false negatives.

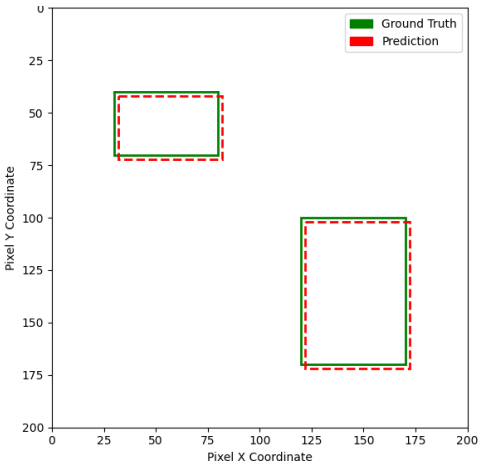

Fig. 3. Bounding Box Refinement, this is a comparison of ground truth (green) and predicted (red) bounding boxes with a better alignment after the DEC-based regression.

The performance trend of the proposed DEC-based bounding box detection model in varying training epochs is presented in Fig. 4. With more and more epochs (20 100), the model steadily increases in all these evaluation measures: accuracy, precision, recall, and F1-score. The model reaches 85.7% accuracy and 83.5% F1-score at 20 epochs and 90.1% accuracy and 87.5% F1-score at 100 epochs. The steady increase proves that the longer the training the more discriminative features the model learns.

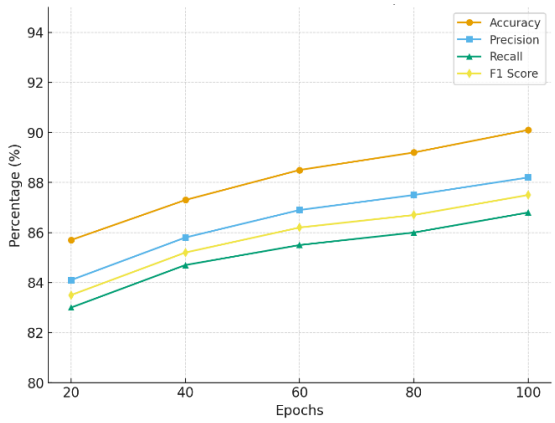

Fig. 4. Performance mertics for proposed approach

B. Comparative Analysis

The comparative analysis with the proposed methods is given with a view of showing the improvements that have been made by this approach. The proposed method is compared with three existing models: YOLOv5, Faster R-CNN and SSD (Single Shot Detector).

Table 2 shows the accuracy performance of the model. The proposed method demonstrates consistent improvement in accuracy over existing methods across all epochs. After 20 epochs, the accuracy of this method is 1.5%–3.2% higher than that of other approaches, suggesting acceleration of the learning process. The proposed method achieves an accuracy of 90.1%, about 2.5% more than the method that performs best overall among those now in use. Improved feature learning, higher detection accuracy, and a drop in false positives all follow from enhanced clustering and bounding box refinement. Strong resilience of the combined clustering and bounding box regression technique is reflected by consistent improvement over time.

Table 2: Accuracy

Epochs	SSD	Faster R-CNN	YOLOv5	Proposed Method
20	82.5%	84.2%	83.1%	85.7%
40	84.0%	85.5%	84.2%	87.3%
60	85.1%	86.4%	85.0%	88.5%
80	85.8%	87.1%	85.7%	89.2%
100	86.3%	87.6%	86.0%	90.1%

Table 3 shows the precision comparison with existing models. Precision of the model in avoiding false positives defines its capacity. With a precision of 88.2% at 100 epochs, 2.6%–3.7% higher than other approaches, the proposed method regularly achieves a better degree of accuracy than other approaches. Improved clustering assignment, which precisely locates cluster centroids so reducing the possibility of erroneous classification, helps to explain the higher precision. Eliminating more vague predictions improves the bounding box refining process and helps to contribute to general increase in accuracy. Consistent increase across an epoch reveals that the model has been able to adapt and raise its detection accuracy over time.

Table 3: Precision

Epochs	SSD	Faster R-CNN	YOLOv5	Proposed Method
20	80.3%	81.5%	82.0%	84.1%
40	82.0%	83.2%	83.5%	85.8%
60	83.1%	84.4%	84.5%	86.9%
80	83.8%	85.0%	84.9%	87.5%
100	84.5%	85.6%	85.3%	88.2%

Table 4 shows the recall comparison. The proposed method achieves higher recall than with the present methods: 86.8% at 100 episodes. This shows a 2.9%–4.3% increase, compared to the other strategies. Combining bounding box refining with clustering assignment helps to improve the detection of true positive cases and so the recall rate. The steady rise in recall implies that the model appears to be effective in improving object coverage in challenging aerial images and reducing missed detections.

Table 4: Recall

Epochs	SSD	Faster R-CNN	YOLOv5	Proposed Method
20	78.0%	79.2%	80.0%	83.0%
40	80.1%	81.3%	81.5%	84.7%
60	81.2%	82.4%	82.3%	85.5%
80	81.8%	83.1%	82.9%	86.0%
100	82.5%	83.7%	83.5%	86.8%

Table 5 represents the F1_Score comparison. By a margin of 3.0%–4.1%, the proposed approach achieves a peak F1-score of 87.5%, which makes it better than the present methods after 100 epochs. The fact that the balanced increase in precision and recall produces an overall F1-score improvement confirms also the robustness of the model's clustering and bounding box refining mechanisms. The fact that the F1-score has been steadily increasing over all epochs indicates that the model is obviously able to find a equilibrium between spotting actual positives and avoiding false positives.

Table 5: F1-Score Comparison

Epochs	SSD	Faster R-CNN	YOLOv5	Proposed Method
20	79.1%	80.3%	81.0%	83.5%
40	81.0%	82.2%	82.5%	85.2%
60	82.1%	83.3%	83.4%	86.2%
80	82.7%	83.9%	83.9%	86.7%
100	83.4%	84.5%	84.3%	87.5%

The hybrid clustering with multi-scale representation provides significant improvements in detecting objects across various scales and backgrounds. By integrating global and local contextual information, the model becomes more adaptive to complex aerial scenes. This approach also reduces false positives and improves localization, offering a scalable solution for practical remote sensing applications.

C. Ablation Study

Ablation study is done on DOTA-v1.0 dataset to assess the suggested DEC loss. The baseline is YOLOv8-s that is trained with conventional CE and IoU losses (70.5 mAP@0.5). Backbone tuning alone produced little effect, since removal of DEC did not lead to differences. The use of KL divergence to introduce DEC resulted in substantially better results (+4.3 mAP@0.5), and thus cluster-driven learning proved to be effective. This last integrated model takes the form of a combination of DEC and KL divergence and IoU loss, with 77.9 mAP 0.5 and 50.3 mAP 0.5:0.95, and the competitive inference speed. This goes to show that the suggested framework promotes accuracy and efficiency when detecting aerial objects. Table 6 shows the results of ablation study.

Table 6: Ablation Study Results on DOTA Dataset

Model Variant	Loss Used	Dataset	mAP@0.5	mAP@0.5:0.95	FPS
Baseline (YOLOv8-s)	CE + IoU	DOTA-v1.0	70.5	44.2	85
Ours w/o DEC	CE + IoU	DOTA-v1.0	72.1	45.0	78
Ours w/ DEC (KL only)	KL divergence only	DOTA-v1.0	74.8	47.6	76
Ours w/ DEC + IoU (final)	KL + IoU (proposed)	DOTA-v1.0	**77.9**	**50.3**	74

* Ours w/o DEC = proposed model without DEC

* Ours w/ DEC (KL only) = proposed model with DEC (KL only)

* Ours w/ DEC + IoU (final) = proposed model with DEC (proposed)

5. Conclusion

Advanced object detection techniques such as multi-scale feature extraction, attention mechanisms, directional object detection, and multimodal data fusion can significantly improve the quality and operational speed of remote sensing systems. These techniques address the various challenges such as scale variation, object localization, and sensor data integration. Applications in ecosystem monitoring, smart city planning, agricultural analysis, and disaster mitigation will improve decision-making, support sustainable development, and improve responses to

global challenges. By leveraging these advances, remote sensing will continue to provide critical information across a wide range of sectors, ensuring better resource management and more informed planning.

Future advancement will focus on several significant technological advancement in remote sensing object detection. Deep learning frameworks, such as more efficient Convolutional Neural Networks (CNN's) and transformer-based models can be enhanced to provide better feature extraction, high performance, and accurate results, especially when dealing with challenging environments. Finally, continuous, real-time monitoring over large areas with minimal human assistance can be enabled with the help of autonomous surveillance systems using AI and machine learning which in turn improves the efficiency and scalability in the applications of urban planning and agriculture. These improvements will provide efficient autonomous remote sensing systems with more accurate and improved performance across a variety of fields.

References

[1] Alhawsawi, A. N., Khan, S. D., & Rehman, F. U. (2024). Enhanced yolov8-based model with context enrichment module for crowd counting in complex drone imagery. Remote Sensing, 16(22), 4175. https://doi.org/10.3390/rs16224175

[2] Anuar, M. M., Halin, A. A., Perumal, T., & Kalantar, B. (2022). Aerial imagery paddy seedlings inspection using deep learning. Remote Sensing, 14(2), 274. https://doi.org/10.3390/rs14020274

[3] Antonakakis, M., Trimas, C., & Zervakis, M. (2023, October). A two-phase ResNet for object detection in aerial images. In 2023 IEEE International Conference on Imaging Systems and Techniques (IST) (pp. 1–5). IEEE. https://doi.org/10.1109/IST59608.2023.10390289

[4] Fagan, J. (2019, March 25). Nursing clinical brain. OER Commons. Retrieved January 7, 2020, from https://www.oercommons.org/authoring/53029-nursing-clinical-brain/view

[5] Gui, S., Song, S., Qin, R., & Tang, Y. (2024). Remote sensing object detection in the deep learning era—a review. Remote Sensing, 16(2), 327. https://doi.org/10.3390/rs16020327

[6] Kalinicheva, E., Sublime, J., & Trocan, M. (2020). Unsupervised satellite image time series clustering using object-based approaches and 3D convolutional autoencoder. Remote Sensing, 12(11), 1816. https://doi.org/10.3390/rs12111816

[7] Li, J., Li, Z., Chen, M., Wang, Y., & Luo, Q. (2022). A new ship detection algorithm in optical remote sensing images based on improved R3Det. Remote Sensing, 14(19), 5048. https://doi.org/10.3390/rs14195048

[8] Li, L., Zhu, X., Ni, S., & Gao, F. (2024, December). Dense object detection for remote sensing images based on multi-scale partitioning and super-resolution optimization. In Proceedings of the 3rd International Conference on Signal Processing, Computer Networks and Communications (pp. 239–245). https://doi.org/10.1145/3639460.3639479

[9] Lin, Q., Zhao, J., Du, B., Fu, G., & Yuan, Z. (2021). MEDNet: Multiexpert detection network with unsupervised clustering of training samples. IEEE Transactions on Geoscience and Remote Sensing, 60, 1–14. https://doi.org/10.1109/TGRS.2021.3112643

[10] Liu, Z., Lin, Y., Cao, Y., Hu, H., Wei, Y., Zhang, Z., Lin, S., & Guo, B. (2021). Swin transformer: Hierarchical vision transformer using shifted windows. In Proceedings of the IEEE/CVF International Conference on Computer Vision (pp. 10012–10022).

[11] Lago, A., Patel, S., & Singh, A. (2024). Low-cost real-time aerial object detection and GPS location tracking pipeline. ISPRS Open Journal of Photogrammetry and Remote Sensing, 13, 100069.

[12] Praghash, K., Arshath Raja, R., Chidambaram, S., & Shreecharan, D. (2022, December). Hyperspectral image classification using denoised stacked auto encoder-based restricted Boltzmann machine classifier. In International Conference on Hybrid Intelligent Systems (pp. 213–221). Cham: Springer Nature Switzerland. https://doi.org/10.1007/978-3-031-20820-0_20

[13] Rajput, K., Suganyadevi, K., Aeri, M., Shukla, R. P., & Gurjar, H. (2024, May). Multi-scale object detection and classification using machine learning and image processing. In 2024 Second International Conference on Data Science and Information System (ICDSIS) (pp. 1–6). IEEE. https://doi.org/10.1109/ICDSIS59739.2024.10403323

[14] Sharma, B., Sharma, A., Sharma, A. M., Thomas, S., & Jamal, A. (2024, July). Object-based analytics for finding homogeneous collections in aerial imagery datasets. In IGARSS 2024-2024 IEEE International Geoscience and Remote

Sensing Symposium (pp. 6959–6963). IEEE. https://doi.org/10.1109/IGARSS55600.2024.10413493

[15] Wang, C. Y., Bochkovskiy, A., & Liao, H. Y. M. (2023). YOLOv7: Trainable bag-of-freebies sets new state-of-the-art for real-time object detectors. In Proceedings of the IEEE/CVF Conference on Computer Vision and Pattern Recognition (pp. 7464–7475).

[16] Yue, M., Zhang, L., Huang, J., & Zhang, H. (2024). Lightweight and efficient tiny-object detection based on improved YOLOv8n for UAV aerial images. Drones, 8(7), 276.

[17] Zhang, H., Li, F., Liu, S., Zhang, L., Su, H., Zhu, J., Ni, L. M., & Shum, H. Y. (2022). DINO: DETR with improved denoising anchor boxes for end-to-end object detection. arXiv preprint arXiv:2203.03605.

[18] Zheng, C., Liu, T., Abd-Elrahman, A., Whitaker, V. M., & Wilkinson, B. (2023). Object-detection from multi-view remote sensing images: A case study of fruit and flower detection and counting on a central Florida strawberry farm. International Journal of Applied Earth Observation and Geoinformation, 123, 103457. https://doi.org/10.1016/j.jag.2023.103457

[19] Zhu, X., Su, W., Lu, L., Li, B., Wang, X., & Dai, J. (2020). Deformable DETR: Deformable transformers for end-to-end object detection. arXiv preprint arXiv:2010.04159.

[20] AID (Aerial Image Dataset). https://paperswithcode.com/dataset/aid